Extracting the angular dependence on cut efficiency of the muon semileptonic final state of W pair decay in the $e_L^- e_R^+$ channel of the ILC

Matthew Koster
University of Cambridge
DESY, Hamburg, Germany
FLC group, Summer Student Programme

September 5, 2019

Supervisor: Jakob Beyer

Abstract

DO ME

Contents

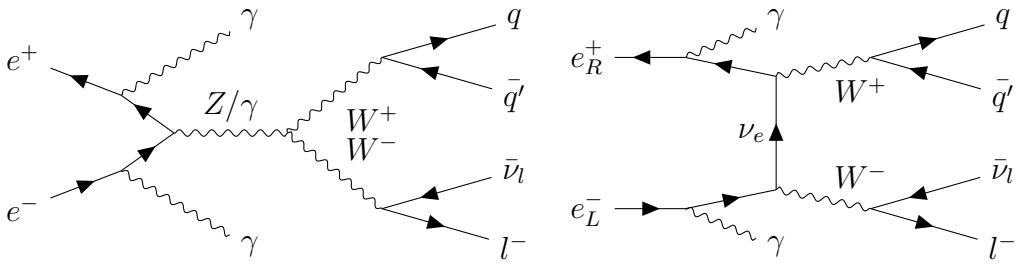

Figure 1: Lowest order Feynman diagram of semileptonic W pair decay in the $\mu\bar{\nu}q\bar{q}'$ final state at e^+e^- colliders, with two ISR photons emitted. Alternately the W^+ could decay leptonically and the W^- hadronically, which would result in a $\mu^+\nu q\bar{q}'$ final state (not drawn).

1 Introduction

DO ME

2 My Processor

2.1 Outline

My processor reconstructs the 4-momenta of the particles in the hard collision from the MC particle collection and the Reconstructed particle collection, and evaluates several variables used in the analysis in Section. 3. In order to do this it must use some kinematically derived formulae (Section. 2.4) to reconstruct the 'invisible 4-momenta contribution of the neutrino and any initial state radiation (ISR). The processor then creates a root file and fills a tree with all of these variables for further analysis. I will now go into more detail on each of the relevant steps.

2.2 Beam Background Removal

In an e^+e^- particle collider, to increase the probability of a hard collision, a 'bunch' [1] of particles are 'collided and due to the low cross-section we may expect only one hard interaction to occur. These other particle, however, do interact with the detector and so will generate so-called beam background. This is modelled in the Monte Carlo simulation of the collision, and so must be removed before analysis of the hard collision can be conducted.

I am using the FastJetProcessor [2] to conduct such beam background removal from the reconstructed particle collection. Another method of background removal is by using the MC particles themselves to remove the background from the reconstructed particles[1], done with the TrueJet processor [3]. This is of course a liberty that is only possible because the collisions are simulated, therefore not possible at an active detector and is therefore referred to in this report as 'cheating overlay removal'. The later method is used to explore the sensitivity of my reconstruction to this beam background removal in Section. 2.5.3.

2.3 4-momenta Reconstruction

For the MC particles, I directly extracted each of the particles in the hard collision from the collection using their element number. Elements 4 and 5 were the ISR photons, 6 and 7 the quarks, 8 the lepton and 9 the neutrino. It was then a simple task of inputting their energies

[1] A different steering file was used for this set up, further discussed in Section. 2.7

and momenta into a TLorentzVector [4]. The W bosons 4-momenta could also simply be calculated by addition of the 4-momenta of its decay products.

Extraction of the 4-momenta of the particles in the hard collision from the Reconstructed particles was done by looping through the particles in the various collections, extracting their momentum and energy, and summing them. The IsolatedLeptonTaggingProcessor [5] returns the hard collision lepton[2], and so summation over this collection reconstructed the 4-momenta of the lepton. The FastJetProcessor returns a colleciton containing the 2 reconstructed quarks, their 4-momenta and subsequently that of the hadronically decaying W boson (W_{had}) can now be similarly reconstructed.

LEP or HAD?? At this point I will mention that re-vertexing did make a difference to the performance of this********

Reconstruction of the leptonically decaying W boson (W_{lep}) requires a bit more thought, this is because of the neutrino and the ISR photons which leave no signal in the detector. This challenge is discussed in detail in the following section.

2.4 Neutrino and ISR Corrections: Implementation

The leptonically decaying W boson can be reconstructed by summing the 4-momenta of the extracted lepton and the neutrino, however, the neutrino does not leave a signal in the detector. There is also some initial state radiation of photons (ISR) which are aligned enough to the beam pipe that they are also not detected. This results in an 'invisible' system that is not at all detected by the detector, we must therefore come up with a way to attain the 4-momenta of these invisible particles if we wish to have complete information about the W bosons.

The chosen method for reconstruction of the invisible system arises purely from conservation laws[3]. We consider the reconstructed visible system as being the hadronically decaying W boson plus the isolated lepton ($p^\mu = (E, p_x, p_y, p_z)$), and the invisible system as the accompanying neutrino and an ISR photon, travelling parallel to the beam. We also assume the total center of mass energy is 500 GeV and that we are in the zero momentum frame (ZMF). Conservation of momentum and energy then gives us the 4-momenta of the ISR photon and the neutrino. In the MC simulation there are actually two ISR photons emitted, this means that when combining the two photons into one 'photon', this 'photon' may have a non zero invariant mass. As well as this, the ISR photon could be going in either direction with respect to the beam axis, resulting in two solutions.

$$E_\gamma = \frac{\lambda(500 - E) \pm p_z\sqrt{\lambda^2 - [(500 - E)^2 - p_z^2]m_\gamma^2}}{(500 - E)^2 - p_z^2} \tag{1}$$

where $\lambda = \frac{1}{2}[(500 - E)^2 - p^2 + m_\gamma^2 - m_\nu^2]$ has been defined for convenience and no absolute values have been assumed.

The solution that gives a better estimate for the invariant mass of the W boson is selected. As described in Ivan's thesis [6] this may shift more of the background into the peak introducing a bias and so the appropriate cut was made to mitigate this.

[2] If it correctly reconstructs the lepton, sometimes it returned zero particles, sometimes more than one, this was cut on later

[3] a full mathematical derivation is included in the appendix for completeness (Appendix. 7.4)

The rest of the unknown variables of momentum and energy are now exactly defined and can be easily evaluated. So we now have the 4-momenta of all of the particles in the hard interaction as required for the analysis.

A simplified form of this equation with $m_\gamma = \pm m_\nu = 0$ is used in Ivan's thesis. Equation. (1) correctly simplifies to this solution as shown in the appendix.

$$E_\gamma = \frac{(500 - E)^2 - p^2}{1000 - 2E \mp 2p_z} \tag{2}$$

It is worth noting at this point that it is numerically possible for the particle reconstruction to result in a visible 4-momenta with a negative λ. It can be seen in the $m_\gamma = m_\nu = 0$ solution that this corresponds to the invisible part of the system having an imaginary invariant mass.

$$\lambda_{m_\gamma, m_\nu = 0} \propto (500 - E)^2 - p^2 = E_{inv}^2 - p_{inv}^2 = m_{inv}^2 \tag{3}$$

When I first ran my processor this occurred in about 22% of the events. This is obviously not physical and will affect the solutions attained above. For example as $p_\gamma = \pm E_\gamma$, a negative energy will reverse the direction of the photon. This needs to be handled carefully in the code to avoid inconsistent solutions and was a bug that resulted in a lot of the further analysis in Section. 2.5

I can analytically show how Equation. 1 leads to Equation. 2 when simplified, there is however one subtlety when this is done computationally. The $\sqrt{\lambda^2}$ will computationally evaluate as $|\lambda|$, so if λ is negative it will in effect reverse the effect of the $\pm$ in Equation. 1 and lead to the opposite solution of the simplified form. So it is clear that these negative λ's may cause some issues if the contribution from the m_γ in non-negligible. I have not explored this further, because in Section. 2.5.2 I show that including the non-zero m_γ contribution from the Monte Carlo has little effect on the solutions attained and so Equation. 2 is used with the $\pm$ swapped accordingly.

2.5 Neutrino and ISR Corrections: Evaluation

Using the method in Section. 2.4 I was able to reconstruct the 4-momentum of the leptonically decaying W boson. As a test of the performance of this chose I chose to look at the reconstructed invariant mass to see how accurately it was reproduced, this is also what Ivan did in his thesis.

Due to the negative ISR photon energies described in the previous section, a bug in my code resulted in a very poorly defined mass peak. What was worse was that I would get a significantly better peak, at around 80 GeV which is close to the currently accepted measurement of 80.3 [7], if I considered the case where there is no ISR at all. Most of the following exploration was conducted to try and identify the cause of the problem. Now that the bug is fixed the results are of interest in testing the sensitivity of the formula to different parameters, these fixed results I will discuss now.

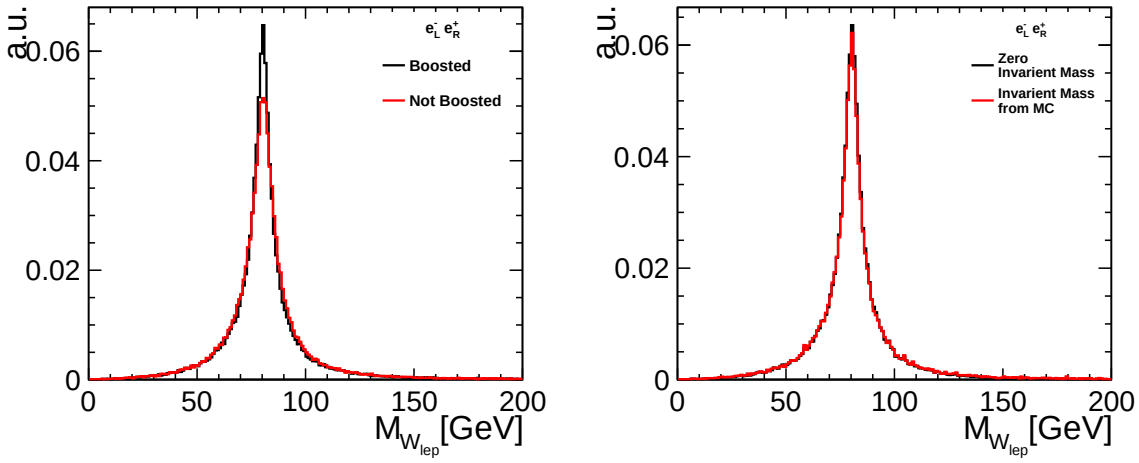

(a) **(b)**

Figure 2: Plots displaying the effect on the reconstructed invarient mass of the leptonically decaying W with different reconstruction methods. The simulated e^+e^- collision is not head on, but with a finite momentum in the x direction, (a) shows the effect of boosting into the ZMF before applying the reconstruction method. (b) shows the effect of inputting a non-zero invarient ISR photon mass into the reconstruction (extracted from the MC collection).

2.5.1 Center of Mass frame

The assumption that the collision is occurring in the centre of mass frame is not trivially satisfied by just reading in the input collection. The e^+e^- collision is incident at a non zero angle, consequently the total system has a non-zero 3-momentum $p^\mu = (500 \sin(\frac{0.014}{2}), 0, 0)$ GeV. This initially was not considered in the analysis because the x-momentum was considered negligible, but in theory addition of a boost into the centre of mass frame should result in an improvement in the reconstruction. In fact we see that is makes a considerable improvement to the mass peak as expected (Figure. 2a) and was kept in the following analysis.

2.5.2 ISR invarient mass

Another assumption that was tested was the non-zero invariant mass of the ISR photon. A quick look at the MC collection revealed that the invariant mass was indeed non-zero for some of the events, and so I investigated how this effected my solutions. I got the invariant mass, from the simulated MC particle collection, by summing the 4-momenta of the 2 extracted photons. Again this is a 'cheat' as this information would not be available to us in a real detector, however I was interested to see the effect it was having on my reconstruction. As can be seen in Figure. 2b, this addition had a negligible effect on the reconstructed W mass. This could be due to the size of the photon mass indeed being negligible, even if non-zero.

2.5.3 Beam Background

The third check I performed was the sensitivity of the reconstructed $m_{W_{lep}}$ to the beam background. I did this by comparing the 2 different background removal methods suggested in Section. 2.2. I found that cheating the beam background removal improved the reconstruction of the 2 quarks, as can be seen in the reconstruction of the invariant mass of the hadronically decaying W boson (Figure. 3). In particular this cheating greatly supresses an overestimation tail observed in the properly reconstructed particles. This in turn improves the reconstruction of the visible portion of the system. The $m_{W_{lep}}$ on the other hand was generally unsensitive

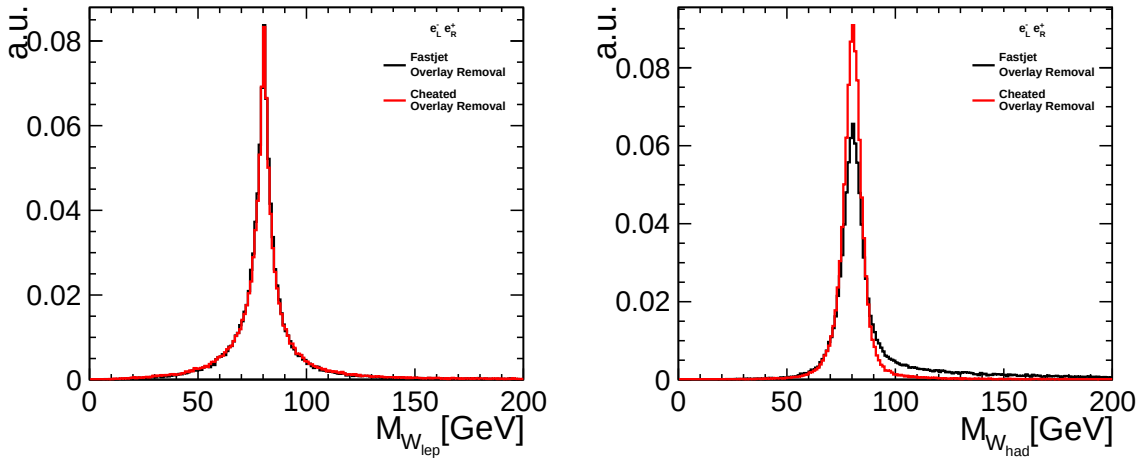

(a) **(b)**

Figure 3: Plots displaying the effect of cheating the beam background removal on the reconstructed invarient mass of the two W bosons, (a) the leptonically decaying W and (b) decaying hadronically.

to this change. Explaining this is non-trivial due to the fairly complicated nature of the E_γ formula.

2.5.4 No ISR

Another place where the formula seemed to be performing poorly was when the true ISR from MC had no or negligible energies. This is shown by Figure. 4a, where the peak is not centered on zero and some considerable overestimations are observed. Before the bug was fixed it also appeared like a solution with no ISR was performing better. Hence I chose to add a third solution to the photon energy formula, where the photon energy, and hence momentum, was set exactly equal to zero. The conservation laws then directly defined the 4-momenta of the neutrino, as it was then the only contribution to the invisible part of the system. As before I calculated the estimate of $m_{W_{lep}}$ using all 3 solutions to E_γ and chose the solution that more accurately reconstructed this mass. Once again this selection may draw more of the background into the peak and introduce a bias. The extent of this is not explored in this report, but it is important to keep into consideration in the following, and any further, analysis. This seems to improve the estimation of $m_{W_{lep}}$ as seen in (Figure. 4b), although I cannot say if this is a true improvement in the method due this bias.

As another check of the performance of this edit I plotted the difference between the reconstructed ISR photon energy and the MC ISR photon energy, to see if this improvement in $m_{W_{lep}}$ was accompanied by an improvement in the estimation of E_γ. To look at this I attempted to created a 'pull' histogram ($\frac{E_\gamma^{Reco}-E_\gamma^{MC}}{E_\gamma^{MC}}$), this returned a fairly large number of divide by zero errors. As the cases with $E_\gamma = 0$ are the ones we are particular interested in this analysis, instead a histogram of just $E_\gamma^{Reco} - E_\gamma^{MC}$ was created (Figure. 4c). Here we can see that the addition of the $E_\gamma = 0$ solution reduces the number of under and over estimates quite significantly. The highest peak at zero is however claimed by the solution where there is no ISR considered at all (green). This means that sometimes an over/under-estimation of the photon energy returns a better reconstruction of the $m_{W_{lep}}$.

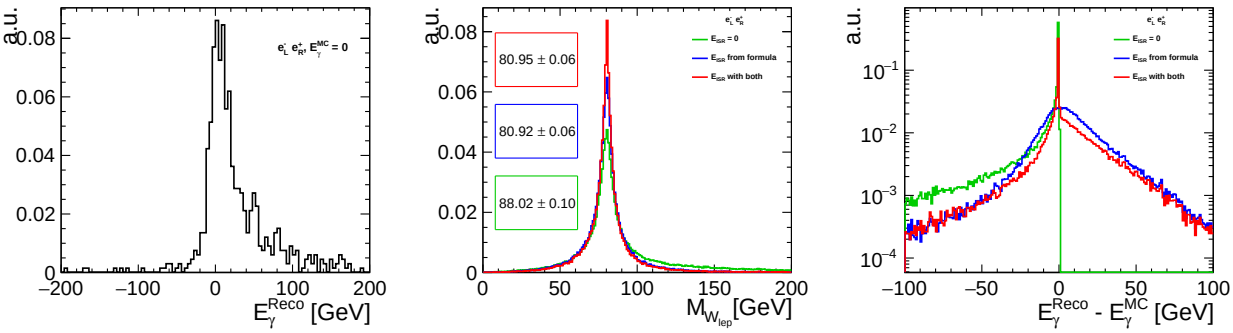

(a) **(b)** **(c)**

Figure 4: (a) displays the reconstructed ISR photon energy from Equation. 2, for cases when the MC ISR energy is zero.
(b) is a histogram showing how well the 3 different E_γ claculation methods reconstruct the leptonically decaying W mass.
(c) is a log histogram plot showing how well the 3 different claculation methods reconstruct E_γ.

2.6 Angle extractions

The final function of my processor is to extract some particular angles of the hard collision from the MC collection, the cut efficiencies of which are the end focus of this report.

The angles are defined in Figure. 5, namely the theta coordinate of the W^- in the centre of mass frame (θ_{W^-}), and the theta and phi coordinates of the lepton in the rest frame of the W_{lep} it decayed from (θ^*_l and ϕ^*_l). The polar coordinate system is the same in both frames, with the z axis aligned to the beam-pipe. The same lorentz boost framework used in Section. 2.5.1 was implemented here and so this was a computationally very simple task, and the extracted angles were put in the root tree.

The resulting angular distributions that I obtained are visible in Figure. 7, where the θ angles have been displayed in terms of their cosine for comparison with Roberts results [8].

2.7 Steering file

In order for Marlin to run my processor correctly, I had to create a 'steering file, which explicitly outlines what Marlin should run, in what order, and the parameters it should input/output at each step. This steering file runs the following processors in order,

- IsolatedLeptonTaggingProcessor
- FastJetProcessor (Beam Background Removal)
- FastJetProcessor (Jet Clustering)
- MyFirstObservableProcessor

This registers the appropriate input collections for my processor, which generates and fills a root file.

The only deviation from this format of steering file was when I cheated the beam background removal. Here I replaced the "FastJetProcessor (Beam Background Removal)" processor with a

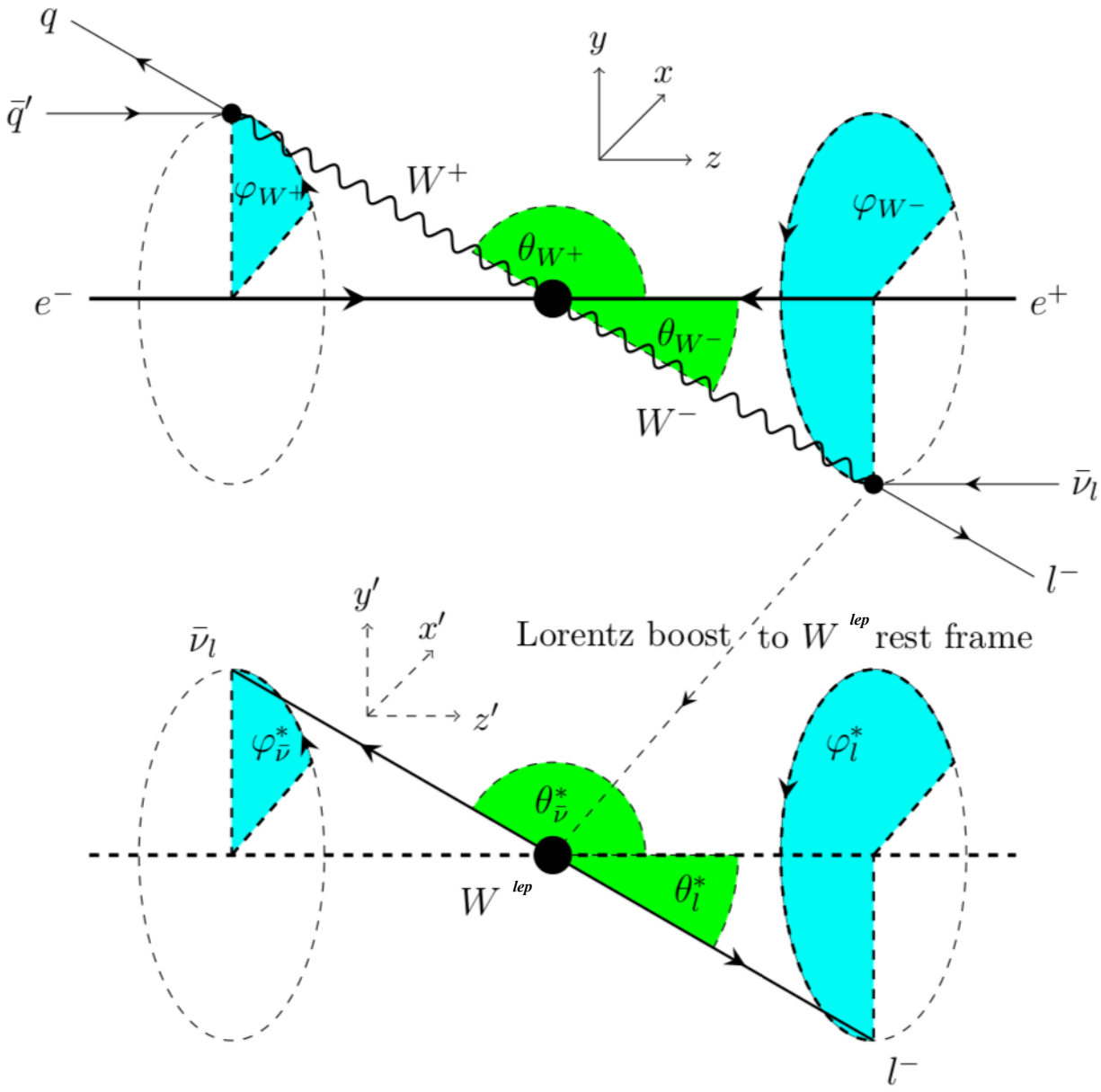

Figure 5: Angle definition for the 4-fermion final state from W^- pair production in the semileptonic channel in which the W decays leptonically. In the top part, the production angles θ_{W^-} and θ_{W^+} are defined by the axis of the initial colliding particles and the direction for the respective boson. The azimuthal angles ϕ_{W^-} and ϕ_{W^+} describe the rotation around the axis of the initial colliding particles.
The bottom picture shows the angular definition of the decay products of the W^{lep} boson in its rest frame. It shows the polar angles θ^*_l and $\theta^*_{\bar{\nu}}$ and the azimuth angles ϕ^*_l and $\phi^*_{\bar{\nu}}$ of the corresponding leptons. The denotes quantities in the rest frame of the W^{lep} boson. (Edited from Robert Karl [8])

"TrueJet"[3] processor followed by a "TJJetRecoParticleFinder"[9] processor. A more detailed description of the inputs and outputs of these processors is given in the Appendix. 7.3

3 Applying Cuts

The following analysis takes places outside of the processor I developed, using python scripts to analyse the data stored in the produced root file. This data was generated by choosing the best of all 3 E_γ solutions, with $m_\gamma = m_\nu = 0$. Unless otherwise explicitly stated, I did not cheat the beam background removal but I did include the boost into the centre of mass frame.

Before any analysis I make sure that I am looking only at the muon signal, as this is the focus of my analysis, by making a cut on the events in MC collection that produced a muon.

3.1 Cut Flow

I sequentially apply all of the same cuts as in Ivans thesis [6] to obtain a cut flow histogram, which tests the efficiency of each of the cuts. This histogram is created by dividing the number of events left after each cut by the initial number of events considered as signal. I can then compare my results to Ivans to see how my processor and the particle reconstruction is performing compared to him. I did this for two different statistical sample sizes, the higher statistics sample being the sample I have used throughout the rest of this report. Further, I created the flow diagram again by cheating the beam background removal, and by applying the additional initial cut that the ISR energy is small ($E_\gamma^{MC} < 1$ GeV). The final plot was made to see if the ISR made a considerable contribution to the efficiency of the cuts.

There are a few subtle differences between the cuts that Ivan and I made, due to the reconstruction methods we implemented. The first was the cut on the jet reconstruction variables y_+ and y_-. I made FastJets reconstruct two jets, corresponding to the 2 quarks, and physically this is the minimum number of jets that occur, as we cannot create a single quark. This means the cut on the y_- variable that Ivan makes is unphysical in my analysis. Ivan applies this cut because he also considered final states with 4 quarks. The lepton cut that I make is also different to Ivans. I am using an IsolatedLeptonTaggingProcessor, and so make the cut that a single isolated lepton is reconstructed. There are a considerable number of events where the processor reconstructs zero particles, and so this cut can be significant. Ivan on the other hand is using a jet reconstruction processor with a specific energy cut to reconstruct isolated leptons. The final difference is that Ivan makes a 'charged lepton' cut, which I cannot see a description of in his thesis. I do not make a similar cut and so the efficiencies of my results will not change in this cut.

For convenience the cuts and efficiencies are tabulated in Table. 1, and the resulting total flow diagram can be seen in (Figure. 6).

[4] track mulitplicity was taken as the number of reconstructed charged particles.

[5] τ_{discr} defined by $\tau_{discr} = \left(\frac{2E_{lep}}{\sqrt{s}}\right)^2 + \left(\frac{m_W^{lep}}{m_W^{true}}\right)^2$

[6] $\Delta\Omega_{iso}$ defined as,

$$(\phi_{lep} - \phi_{had}) < \pi \rightarrow \Delta\Omega_{iso} = \sqrt{(\theta_{lep} - \theta_{had})^2 + (\phi_{lep} - \phi_{had})^2} \tag{4}$$

$$(\phi_{lep} - \phi_{had}) \geq \pi \rightarrow \Delta\Omega_{iso} = \sqrt{(\theta_{lep} - \theta_{had})^2 + (2\pi - |\phi_{lep} - \phi_{had}|)^2}\,. \tag{5}$$

Table 1: Selection efficiency of sequantially applied cuts. Where the post ISR correction m_W^{lep} was calculated using all 3 possible E_γ solutions. (*) Indicates cuts where my and Ivan's cuts differ, as discussed in the text.

Order	Cut description	Efficiency [%]			
		My Results			Ivan's Results
		n = 2129	n = 99419		n = 107233
			no cheat	cheat	
0	muon signal	100.00	100.00	100.00	100.00
1	track multiplicity[4] $n_{tracks} \geq 10$	97.13	97.01	96.23	99.996
2	center of mass energy $\sqrt{s} > 100$ GeV	92.29	91.69	84.35	97.96
3	total transverse momentum $P_T > 5$ GeV	91.16	90.47	83.28	96.69
4	total energy $E_{SUM} < 500$ GeV	89.66	89.28	82.70	95.36
5	$\ln(y_+) \in [-12, -3]$ (*)	88.69	88.08	82.47	95.01
6	1 lepton found (*)	80.65	80.77	81.50	78.75
7	pre ISR correction $m_W^{lep} \in [20, 250]$ GeV	78.23	77.94	77.84	76.61
8	tau discrimination[5]	76.05	75.60	75.73	74.07
9	charged lepton (*)	76.05	75.60	75.73	73.51
10	isolation variable[6] $\Delta\Omega_{iso} > 0.5$	76.01	75.58	75.72	73.42
11	post ISR correction $m_W^{lep} \in [40, 120]$ GeV	72.90	72.77	72.33	70.13
12	post ISR correction $m_W^{had} \in [40, 120]$ GeV	63.21	62.92	70.52	66.93
13	$\cos\theta_W > -0.95$	63.02	62.65	70.21	66.78

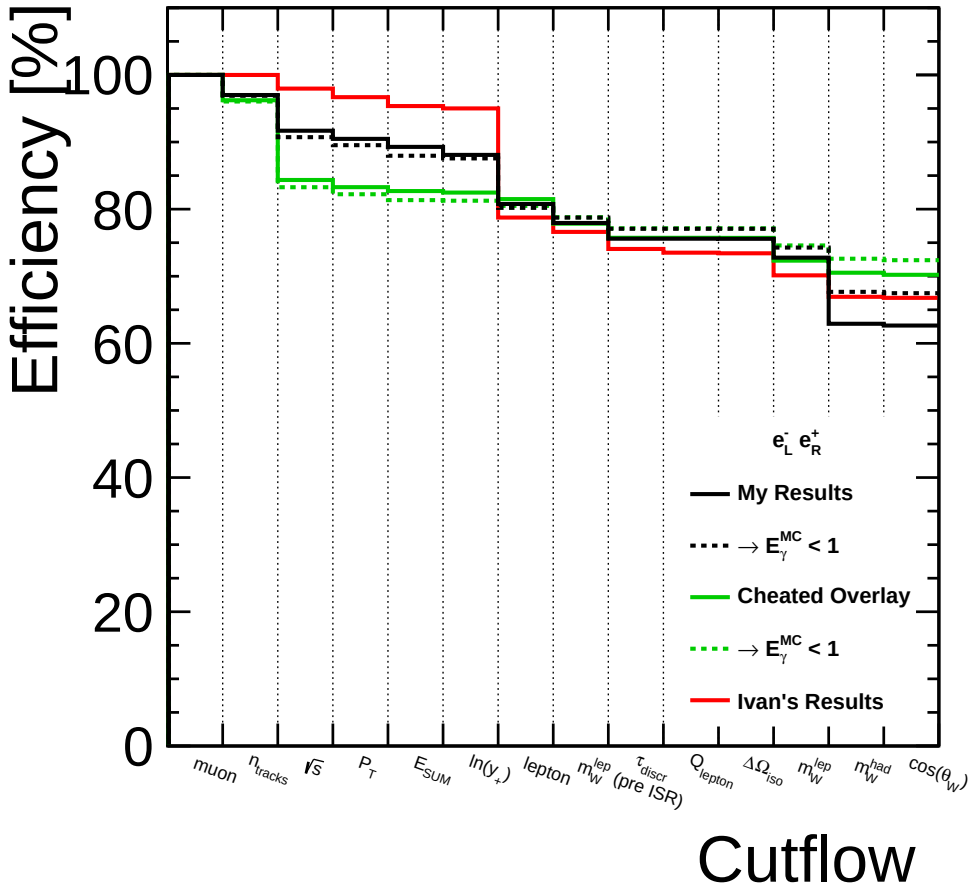

Figure 6: Histograms showing the cut flows for Ivan's results, my results (with and whithout cheating overlay removal), and my results again when the ISR photon has low energy ($E_\gamma < 1$). The cuts on the x axis are as defined in Table. 1.

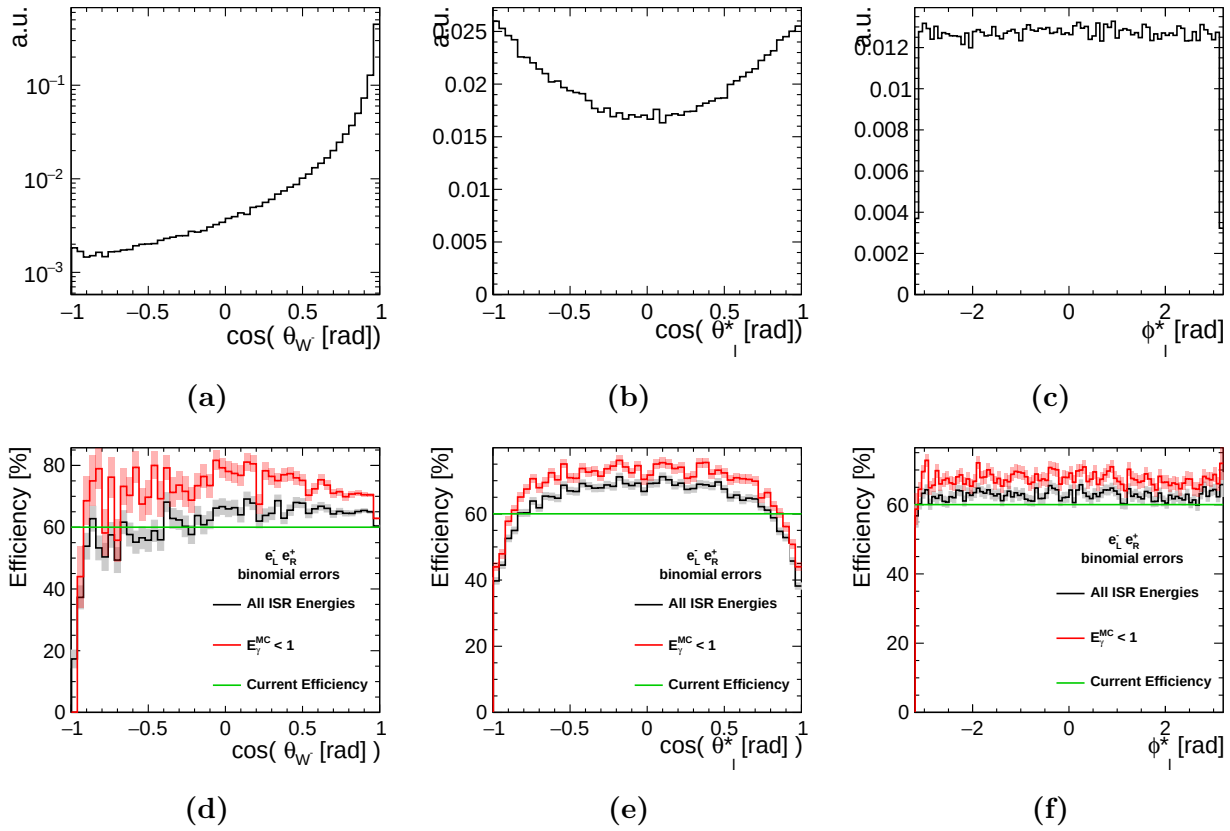

Figure 7: (a), (b) and (c) are the extracted angles as defined in Figure. 5.
(d), (e) and (f) are the associated cut efficiencies, after applying the cuts outlined in Table. 1.

We can see a fairly large difference in the cut efficiencies before the lepton cut. I believe this is because, for me, the cut on finding only one isolated lepton would make a considerable difference to the performace of the reconstruction. In all of the events where no isolated leptons were reconstructed the leptonic W boson is reconstructed entiely from the invisble neutrino, which will be completely wrong. We see that 'My Results' and the 'Cheated Overlay' reconverge on this lepton cut and I believe this is because the differences prior were caused by such events. I have not explored this further in this report, a check would be to perform the lepton cut first and see how the two historgams differ then.

After the lepton cut, we can see that my results are generally performing better than Ivan's, untill the cut on the m_W^{had} where it is considerably worse. By looking at the cheated results though we can see that this is apparently due to the beam background. We also see that after the lepton cut the $E_\gamma^{MC} < 1$ GeV is consistently performing better than the full signal, which suggests that large ISR energies worsens the performance of the reconstruciton.

3.2 Angle Cut Efficiencies

I can now complete the end goal of my report, to evaluate the angular dependancy of the cut efficiency. This can be done by dividing an angular distribution histogram with all of the perviously defined cuts applied, by the same histogram where the only applied cut is that we are looking at a muon signal. I did this for both the full signal and the $E_\gamma^{MC} < 1$ GeV signal, which can be seen in Figure. 7.

The $\cos(\theta_{W^-})$ plot can be seen to be fairly statistically limited towards -1, in the backwards

direction, and this greatly reduces the efficiency here, it is however reasonably constant throughout the rest of the distribution. The $\cos(\theta_l^*)$ appears to have a poor efficiency in regions closely aligned to the beam-pipe. This is as expected due to ***FILL ME****. ϕ_l^* has a uniform efficiency as well as angular distribution. This is to be expected because there is no initial phi momentum that could bias this result. Even though the lepton's angle will have a dependance on that of the W boson it decayed from, this W boson will be uniformly distributed in phi and so we expect the same from the lepton. This may not be the case if the stared (*) coordinate system what oriented such that $\phi_l^* = 0$ lied in the plane defined by the beam axis and the W boson, but that has not been explored in this report.

The $E_\gamma^{MC} < 1$ GeV signal performed very similarly to the full signal, but the magnitude of the efficiency seemed to be different by a reasonably consistent factor.

4 Conclusion

DO ME

5 References

[1] F Jet. In: ().

[2] F Jet. In: ().

[3] T Jet. In: ().

[4] T Lorentz. In: ().

[5] I Tag. In: ().

[6] I Marchesini. In: ().

[7] R Karl. In: ().

[8] R Karl. In: ().

[9] T JJet. In: ().

6 Acknowledgments

7 Appendix

7.1 Log Figures

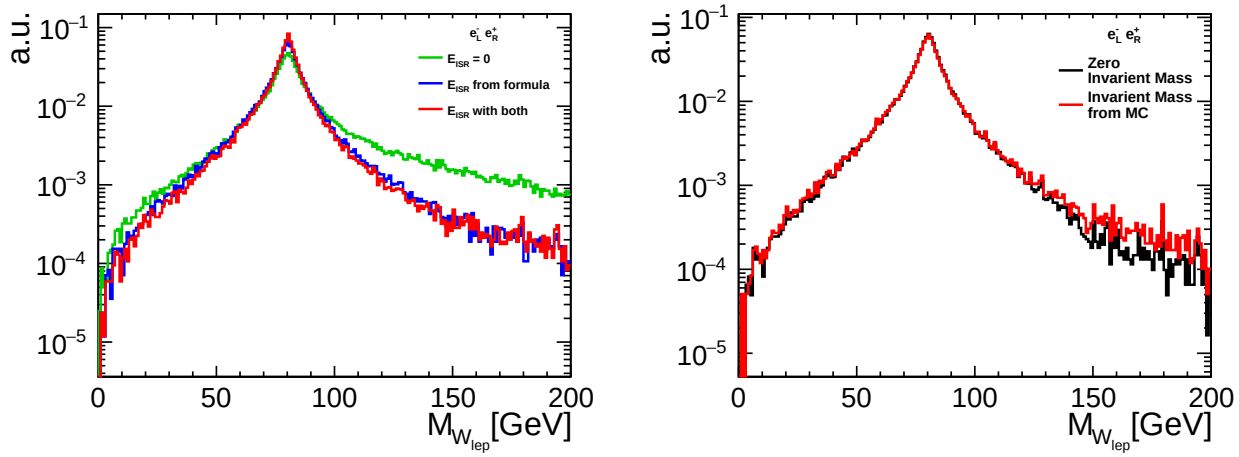

7.2 Steering file

The layout of my steering file:

- IsolatedLeptonTaggingProcessor
  - InputCollection: PandoraPFOs
  - Electron Weight: /cvmfs/ilc.desy.de/sw/x86_64_gcc49_sl6/v02-00-02/MarlinReco/v01-25/Analysis/IsolatedLeptonTagging/weights/yyxyev_yyxyyx_500.mILD_l5_o1_v02
  - Muon Weight: /cvmfs/ilc.desy.de/sw/x86_64_gcc49_sl6/v02-00-02/MarlinReco/v01-25/Analysis/IsolatedLeptonTagging/weights/yyxylv_yyxyyx_woYoke_500.mILD_l5_o1_v02
  - OutputCollection: Isoleps
  - OutputCollection: PFOsWithoutIsoleps
- FastJetProcessor (Beam Background Removal)
  - InputCollection: PFOsWithoutIsoleps
  - OutputCollection: PFOsOverlayRemoved
- FastJetProcessor (Jet Clustering)
  - InputCollection: PFOsOverlayRemoved
  - OutputCollection: FastJets
  - OutputCollection: PFOsFromFastJet
- MyFirstObservableProcessor
  - InputCollection: MCParticle
  - InputCollection: PFOsOverlayRemoved
  - InputCollection: Isoleps

- InputCollection: FastJets

with LCIO input files:
/pnfs/desy.de/ilc/prod/ilc/mc−opt−3/ild/dst−merged/500−TDR_ws/4f_WW_semileptonic/ILD_l5_o1_v02/v02−00−01/rv02−00−01.sv02−00−01.mILD_l5_o1_v02.E500−TDR_ws.I250018.P4f_ww_sl.eL.pR.n0 ∗ .d_dstm_10318_ ∗ .slcio.

The only deviation from this format of steering file was when I cheated the beam background removal. Here I replaced the "FastJetProcessor (Beam Background Removal)" processor with a "TrueJet" processor with MCParticle input collection followed by a "TJJetRecoParticleFinder" processor which outputs a collection RecosFromHadronicJets. This RecosFromHadronicJets collection was then used as the input to the "FastJetProcessor (Jet Clustering)" processor.

- IsolatedLeptonTaggingProcessor
  - InputCollection: PandoraPFOs
  - Electron Weight: /cvmfs/ilc.desy.de/sw/x86_64_gcc49_sl6/v02−00−02/MarlinReco/v01−25/Analysis/IsolatedLeptonTagging/weights/yyxyev_yyxyyx_500.mILD_l5_o1_v02
  - Muon Weight: /cvmfs/ilc.desy.de/sw/x86_64_gcc49_sl6/v02−00−02/MarlinReco/v01−25/Analysis/IsolatedLeptonTagging/weights/yyxylv_yyxyyx_woYoke_500.mILD_l5_o1_v02
  - OutputCollection: Isoleps
  - OutputCollection: PFOsWithoutIsoleps
- TrueJet
  - InputCollection: MCParticle
- TJJetRecoParticleFinder
  - OutputCollection: RecosFromHadronicJets
- FastJetProcessor (Jet Clustering)
  - InputCollection: RecosFromHadronicJets
  - OutputCollection: FastJets
  - OutputCollection: PFOsFromFastJet
- MyFirstObservableProcessor
  - InputCollection: MCParticle
  - InputCollection: PFOsOverlayRemoved
  - InputCollection: Isoleps
  - InputCollection: FastJets

7.3 Derivation of the ISR energy E_γ with non-trivial m_γ and m_ν

Our initial assumptions are that the system is in the center of mass frame with an invariant mass of 500 GeV. The system contains a visible 4-momentum $p^\mu = (E, p_x, p_y, p_z)$ and an invisible 4-momentum (a neutrino $p^\mu_\nu = (E_\nu, p_{\nu,x}, p_{\nu,y}, p_{\nu,z})$ and an ISR photon $p^\mu_\gamma = (E_\gamma, 0, 0, p_\gamma)$). Both the neutrino and the photon have a non trivial invariant mass leading to the following equations.

Conservation of 3-momentum

$$p_x + p_{\nu,x} = 0 \tag{6}$$
$$p_y + p_{\nu,y} = 0 \tag{7}$$
$$p_z + p_{\nu,z} + p_\gamma = 0 \tag{8}$$
$$\tag{9}$$

Conservation of Energy

$$E + E_\nu + E_\gamma = 500 \tag{10}$$

Energy-Momentum equations

$$E_\nu^2 = p_\nu^2 + m_\nu^2 \tag{11}$$
$$E_\gamma^2 = p_\gamma^2 + m_\gamma^2 \tag{12}$$
$$\tag{13}$$

For a unique solution of E_γ we require 2 more constraints on m_γ and m_ν which have yet to be imposed, but assuming these constraints are independent of E_γ we can arrive at a solution as follows.

From conservation of 3-momentum

$$\begin{aligned} p_\nu^2 &= p_{\nu,x}^2 + p_{\nu,y}^2 + p_{\nu,z}^2 && (14)\\ &= p_x^2 + p_y^2 + (p_\gamma + p_z)^2 && (15)\\ &= p^2 + p_\gamma^2 + 2p_\gamma p_z && (16)\\ &= p^2 + E_\gamma^2 - m_\gamma^2 + 2p_\gamma p_z\,. && (17) \end{aligned}$$

Conservation of energy then gives us,

$$\begin{aligned} (500 - E)^2 - p^2 &= (E_\nu + E_\gamma)^2 - p^2 && (18)\\ &= E_\nu^2 + E_\gamma^2 - p^2 + 2E_\gamma E_\nu && (19)\\ &= p_\nu^2 + m_\nu^2 + E_\gamma^2 - p^2 + 2E_\gamma E_\nu\,. && (20) \end{aligned}$$

Substituting in the expression for p_ν,

$$\begin{aligned} (500 - E)^2 - p^2 &= \cancel{p^2} + E_\gamma^2 - m_\gamma^2 + 2p_\gamma p_z + m_\nu^2 + E_\gamma^2 - \cancel{p^2} + 2E_\gamma E_\nu && (21)\\ (500 - E)^2 - p^2 + m_\gamma^2 - m_\nu^2 &= 2(E_\gamma^2 + p_\gamma p_z + E_\gamma E_\nu) && (22)\\ &= 2(\cancel{E_\gamma^2} + p_\gamma p_z + E_\gamma[500 - \cancel{E_\gamma} - E]) && (23)\\ &= 2(p_\gamma p_z + 500E_\gamma - EE_\gamma)\,. && (24) \end{aligned}$$

Where we have one again used conservation of energy.

For convenience lets define

$$\lambda = \frac{1}{2}[(500 - E)^2 - p^2 + m_\gamma^2 - m_\nu^2] \tag{25}$$

and use $E_\gamma^2 = p_\gamma^2 + m_\gamma^2$ to arrive at a solvable equation in E_γ .

$$\lambda = p_\gamma p_z + 500E_\gamma - EE_\gamma \tag{26}$$
$$[\lambda - (500 - E)E_\gamma] = p_\gamma p_z \tag{27}$$
$$[\lambda - (500 - E)E_\gamma]^2 = (E_\gamma^2 - m_\gamma^2)p_z^2 \tag{28}$$
$$\lambda^2 - 2\lambda(500 - E)E_\gamma + (500 - E)^2{E_\gamma}^2 = p_z^2E_\gamma^2 - p_z^2m_\gamma^2 \tag{29}$$
$$[(500 - E)^2 - p_z^2]E_\gamma^2 - 2\lambda(500 - E)E_\gamma + (\lambda^2 + p_z^2m_\gamma^2) = 0 \tag{30}$$

This can be solved with the quadratic formula to give,

$$E_\gamma = \frac{\lambda(500 - E) \pm \sqrt{\lambda^2(500 - E)^2 - [(500 - E)^2 - p_z^2][\lambda^2 + p_z^2m_\gamma^2]}}{(500 - E)^2 - p_z^2} \tag{31}$$
$$= \frac{\lambda(500 - E) \pm p_z\sqrt{\lambda^2 - [(500 - E)^2 - p_z^2]m_\gamma^2}}{(500 - E)^2 - p_z^2}\,. \tag{32}$$

As expected, the solution with $m_\gamma = m_\nu = 0$ reduces to the previously calculated solution

$$\lambda = \frac{1}{2}[(500 - E)^2 - p^2 + \cancelto{0}{m_\gamma^2} - \cancelto{0}{m_\nu^2}] \tag{33}$$
$$E_\gamma = \frac{\lambda(500 - E) \pm p_z\sqrt{\lambda^2 - [(500 - E)^2 - p_z^2]\cancelto{0}{m_\gamma^2}}}{(500 - E)^2 - p_z^2} \tag{34}$$
$$= \frac{\lambda[(500 - E) \pm p_z]}{(500 - E)^2 - p_z^2} \tag{35}$$
$$= \frac{\frac{1}{2}[(500 - E)^2 - p^2]}{(500 - E) \mp p_z} \tag{36}$$
$$= \frac{(500 - E)^2 - p^2}{1000 - 2E \mp 2p_z}\,. \tag{37}$$

c.f Ivan's result [6]

It can also easily be shown for this case that the two solutions correspond to ISR photons travelling parallel or anti-parallel to the z axis. The $\mp$ in the denominator hence corresponds to the sign of the photons z momentum,

$$E_\gamma = \frac{(500 - E)^2 - p^2}{1000 - 2E + 2sgn(p_\gamma)p_z} \tag{38}$$

$$E_\gamma = \frac{\lambda(500 - E) + sgn(p_\gamma)p_z\sqrt{\lambda^2 - [(500 - E)^2 - p_z^2]m_\gamma^2}}{(500 - E)^2 - p_z^2}\,. \tag{39}$$